# Klein tunnelling model of low energy electron field emission from single-layer graphene sheet

S. Sun,[1] L. K. Ang,[1,a)] D. Shiffler,[2] and J. W. Luginsland[3]
[1]*School of Electrical and Electronic Engineering, Nanyang Technological University, Singapore 639798*
[2]*Air Force Research Laboratory, Kirtland Air Force Base, New Mexico 87117, USA*
[3]*Air Force Office of Scientific Research, Arlington, Virginia 22203, USA*

(Received 4 May 2011; accepted 21 June 2011; published online 7 July 2011)

By considering the effect of Klein tunneling for low energy electrons with linear energy dispersion, a model has been constructed to calculate the amount of emitted line current density from a single-layer graphene sheet, which is vertically aligned inside a dc gap. It is found that the current-voltage scaling obtained from the constructed Klein tunneling model is very different from the traditional field emission model based on the Fowler-Nordheim (FN) law. Under the same geometrical field enhancement factor, our model predicts a much higher emitted current as compared to the FN law at low voltages. © *2011 American Institute of Physics*. [doi:10.1063/1.3609781]

Since the first single-layer graphene was isolated in 2004,[1] it has rapidly become a hot research area due to its unique electronic properties and applications.[2] Recently, there have been significant interests in using graphene or graphene composite as an efficient electron source, because of low turn on voltage,[3,4] high current density,[3,5] good stability,[5–7] long lifetime,[8] and compactness in a nanogap.[9]

However, all the reported experimental findings[3–9] have treated graphene as a bulk material and used the traditional Fowler-Nordheim (FN) law[10] to fit the experimental results by assuming a field enhancement factor $\beta$. This approach is not appropriate due to the fact that graphene is a two-dimensional superlattice, which is very different from a traditional bulk material assumed in the derivation of the FN law. For graphene, the low energy electrons near the corners of the hexagonal Brillouin zone have a linear energy dispersion, mimicking the massless Dirac fermion, which exhibit angle-dependent Klein tunneling phenomenon[11,12] leading to a much higher tunneling coefficient as compared to the FN law. Thus, the high current emission from graphene may be due to Klein tunneling, in addition to the large field enhancement assumed in the previous studies.

Before presenting our model, it is worthwhile to estimate the value of $\beta$ for a single-layer graphene sheet. If we consider a single-layer graphene sheet as a knife-edge field emitter with a height of $H$ and a width of $2a = 0.335$ nm (see Fig. 1(a)), $\beta$ can be calculated by $\sqrt{(\pi H)/(4a)}$ for $H \gg a$.[13] For $H = 1$ to 10 $\mu$m, $\beta$ is about 70 to 220, which is much smaller than the reported values obtained from fitting the measurements with the FN law, such as $\beta = 3000$ for few layers of graphene,[4] $\beta = 1200$ for graphene composite,[8] and $\beta > 10\,000$ for doped graphene.[3] Thus, the reported high current emission at low turn-on voltage from graphene may not simply due to large field enhancement, but other reasons that are not captured by the traditional FN law. In this paper, we are interested to include the effects of linear energy dispersion and Klein tunneling for electron field emission from a single-layer vertically aligned graphene sheet. We will show later that our model provides a different current-voltage scaling and also a much higher current emission as compared to the FN law. Note vertically well-aligned graphene single layer considered here has been recently fabricated in arrays with $H$ from 50 to 800 nm.[14]

In our model, we assume a single-layer graphene with height $H$ vertically aligned (along x-axis) inside a dc gap of spacing $D \gg H$ with an applied voltage of $V_g$ as shown in Fig. 1(a). The graphene sheet has a width of $2a = 0.335$ nm (along z-axis) and a length of $L$ (along y-axis), where $L$ is assumed to be infinitely long so that the boundary condition (zig-zag or armchair) on the graphene edge could be ignored. By including the effects of linear energy dispersion and

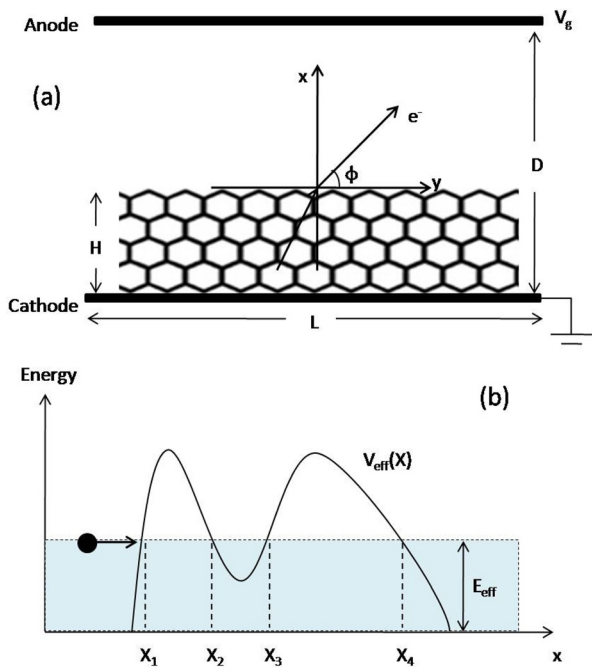


FIG. 1. (Color online) (a) Klein-tunneling field emission model of vertically aligned single-layer graphene sheet, where $V_g$ is the applied voltage bias between the anode and the cathode, $D$ is the gap spacing, $L$ and $H$ ($\ll D$) are the length and height of the graphene sheet, respectively. (b) Effective potential profile $V_{eff}$ of a dual-barrier for an electron with an effective energy $E_{eff}$, and $x_1$, $x_2$, $x_3$, $x_4$ are the four corresponding turning points at $E_{eff} = V_{eff}$.

a)Author to whom correspondence should be addressed. Electronic mail: elkang@ntu.edu.sg.

 

Klein tunneling, the emitted electron current line density $J_L$ (in unit of A/m) can be calculated by

$$J_L = \frac{e}{2\pi^2\hbar^2 v_F}\int_0^{E_0}\int_{-\pi/2}^{\pi/2} T_c(E,\phi)f(E)Ecos\phi \cdot dE \cdot d\phi, \quad (1)$$

where $e$ is the electron charge, $\hbar$ is the reduced plank constant, $v_F = 1\times10^6$ m/s is the Fermi-velocity of graphene, $f(E)$ is the Fermi-Dirac distribution, and $T_c$ is the Klein tunneling coefficient, which is a function of electron energy $E$ and incident angle $\phi$ (in x-y plane). In the derivation of Eq. (1), we have considered that graphene is a two-dimensional structure, so that the integrand is in the form of $dk_x \cdot dk_y$ as compared $dk_x \cdot dk_y \cdot dk_z$ for a bulk material. The second consideration is to apply the linear energy dispersion $E = \hbar v_F k$ instead of $E = \frac{\hbar^2k^2}{2m}$ Note Eq. (1) remains valid as long as the electron energy $E$ is small so that the linear energy dispersion $E = \hbar v_F k$ is maintained, and the Klein tunneling effect is important. In our calculations shown below, we have assumed $E_f = 0.1$ eV (unless it is specified), and the upper limit of the integration $E_0$ (= 0.5 eV) is set to 5 times higher than $E_f$ to avoid numerical errors.

The most difficult part in solving Eq. (1) is to calculate the Klein tunneling probability $T_c$ because it will require solving the Dirac equation. Previous works[12] mainly focused on Klein tunneling through a square barrier as it is relatively easy to find an analytical solution. However, for field emission, the potential barrier is in a form of $V(x) = V_0 - F\cdot x - Q/x$, where $F = \beta F_o$ is the local electric field, $F_o$ is the applied field ($= V_g/D$), $V_0 = 4.66$ eV is set to be the work function of graphene, and $Q/x$ is the image-charge potential with $Q = e^2/(4\pi\varepsilon_0)$ is a constant.[15] Using this $V(x)$, we will calculate $T_c$ based on a relativistic WKB method that was recently developed for Dirac equation.[16,17]

Starting with the Dirac equation $\hat{H}\Psi = E\Psi$, the Hamiltonian of graphene is expressed as $\hat{H} = v_F \cdot (\delta_x p_x + \delta_y p_y) + V(x)$, where $\delta_x$ and $\delta_y$ are the Pauli's matrices, $p_x = -i\hbar\frac{\partial}{\partial x}$ and $p_y = -i\hbar\frac{\partial}{\partial y}$ are the momentum operators, and $V(x)$ is the potential barrier mentioned above. By considering the conservation of the transverse momentum in y-direction, a solution in the form of $\Psi = e^{ik_y y}\cdot\begin{pmatrix}\psi_A(x)\\ \psi_B(x)\end{pmatrix}$ can be substituted into the Dirac equation to find an expression of wavevector $q$. In doing so, we can rewrite the Dirac equation into two coupled differential equations: $\psi'_{A,B} = \frac{d}{dx}\begin{bmatrix}\psi_A(x)\\ \psi_B(x)\end{bmatrix} = \frac{1}{\hbar v_F}\cdot\Lambda\cdot\psi_{A,B}$, where $\Lambda$ is a matrix given by

$$\Lambda = \begin{pmatrix}\hbar v_F k_y & -i(V(x)-E)\\ i(V(x)-E) & -\hbar v_F k_y\end{pmatrix}. \quad (2)$$

Following a series of formulations,[17] the wave vector in the WKB form can be found, respectively, as $q = \sqrt{(\hbar v_F k_y)^2 - (V(x)-E)^2}$, and $q = i\sqrt{(V(x)-E)^2 - (\hbar v_F k_y)^2}$, for $(\hbar v_F k_y)^2 - (V(x)-E)^2 \geq 0$, and $(\hbar v_F k_y)^2 - (V(x)-E)^2 < 0$, which indicate the classical forbidden and allowed region.

In solving Eq. (1) numerically, we define an effective energy of $E_{eff} = \hbar v_F k_x = Ecos\,\phi$ (which is the actual amount of energy incident on the barrier in x-direction) and an effective potential of $V_{eff} = E_{eff} + \sqrt{(\hbar v_F k_y)^2 - (V(x)-E)^2}$ and $V_{eff} = E_{eff} - \sqrt{(V(x)-E)^2 - (\hbar v_F k_y)^2}$, respectively, for $V_{eff} \geq E_{eff}$ (classical forbidden region) and $V_{eff} < E_{eff}$ (classical allowed region). In doing so, we have transformed the original angle-dependent tunneling problem into a one-dimensioonal (1D) dual-barrier tunneling problem [as shown in Fig. 1(b)] with its four corresponding turning points (determined at $V_{eff} = E_{eff}$), which are

$$\begin{cases} x_1 = \dfrac{V_0 - E(1+\sin\phi) - \sqrt{(V_0 - E(1+\sin\phi))^2 - 4FQ}}{2F},\\ x_2 = \dfrac{V_0 - E(1+\sin\phi) + \sqrt{(V_0 - E(1+\sin\phi))^2 - 4FQ}}{2F},\\ x_3 = \dfrac{V_0 - E(1-\sin\phi) - \sqrt{(V_0 - E(1-\sin\phi))^2 - 4FQ}}{2F},\\ x_4 = \dfrac{V_0 - E(1-\sin\phi) + \sqrt{(V_0 - E(1-\sin\phi))^2 - 4FQ}}{2F}. \end{cases} \quad (3)$$

Using Eq. (3), we determine the turning points as a function of $\phi$ and $F$ and solve for the Klein tunneling coefficient $T_c$ based on a standard tunneling problem through a dual-barrier.[18] The calculated $T_c$ are plotted in Fig. 2(a) for various local field $F$ (V/nm) = 0.01, 0.1, 1, and 10 (left to right). As expected, we have perfect transmission ($T_c = 1$) at normal incidence ($\phi = 0°$), and it decreases to 0 at large $\phi$ approaching 90°. Compared to the analytical results of Klein tunneling through a square barrier,[12] the continuously varying potential barrier $V(x)$ that we used here will remove other resonance angles with perfect transmission except at $\phi = 0°$. The figure also shows that the overall tunneling effect

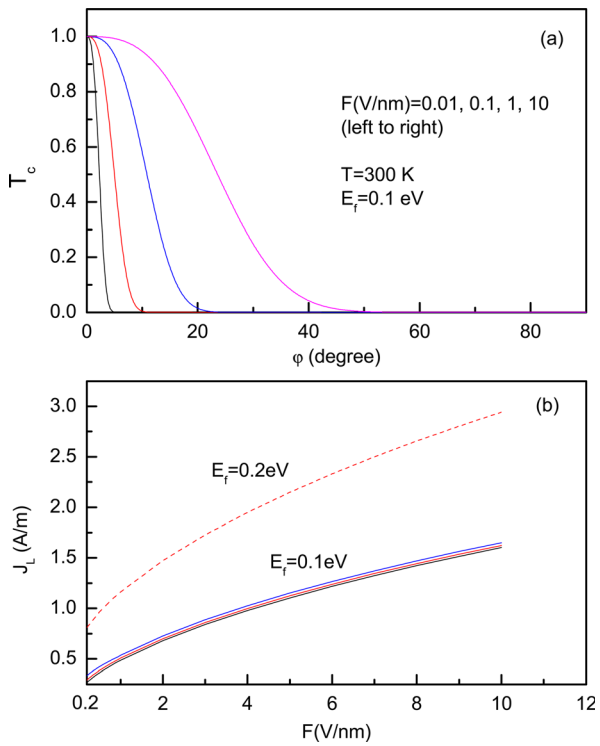


FIG. 2. (Color online) (a) Klein tunneling coefficient $T_c$ as a function of incident angle $\phi$ at various local electric field $F$. (b) The emission line current density $J_L$ as a function of local field $F$ for $E_f = 0.1$ eV (solid lines) at temperature $T$ [K] = 500, 300, 100 (top to bottom), and $E_f = 0.2$ eV (dashed line) at 300 K.

increases (the area under the curve increases) due to the reduction of the barrier's height and width with increasing of local field from $F = 0.01$ V/nm to 10 V/nm.

By substituting $T_c$ into Eq. (1), we calculate the field emission current line density $J_L$ (A/m) as a function of local electric field $F = 0.2$ to 10 V/nm at $E_f = 0.1$ eV (solid lines) as shown in Fig. 2(b). If one assumes a field enhancement of $\beta = 200$ (for a graphene sheet with a height of $H = 10$ $\mu$m), this corresponds to a low turn-on applied field $F_o = F/\beta$ ranging from $F_o = 1$ to 50 V/$\mu$m with a high current line density (0.3 to 1.5 A/m). Our model is also showing a current-voltage (J-F) scaling that is very different from the traditional FN law [$J_{FN} = AF^2\exp(-F/B)$] and also has a much higher current at small $F < 5$ V/nm. For example, at $F = 1$ V/nm, our model gives about $J_L = 0.5$ A/m, while line current density based on FN law [$J_{FN} \times (2a)$] is infinitely small. At higher $F = 5$ V/nm, our calculated result is $J_L = 1$ A/m, as compared to $J_{FN} \times (2a) = 0.81$ A/m. This unusual behavior clearly indicates that when the low energy electrons of the graphene are treated as massless Dirac fermion, the effect of Klein tunneling will greatly affect the current-voltage scaling, and it cannot be explained by FN law. The increment of $J$ at higher temperature $T$ can also be seen when we use $T = 500$, 300, and 5 K (solid line: top to bottom). A calculation with a higher value of $E_f = 0.2$ eV (dashed line) at 300 K is also plotted for comparison.

In Fig. 3, we also present the normalized energy distribution of the emitted electron at various values of (a) local field $F$, (b) temperature $T$, and (c) Fermi energy $E_f$. The normalized constant is the peak value obtained at $F = 0.01$ V/nm, $T = 300$ K, and $E_f = 0.1$ eV (plotted in solid lines). By increasing $F$ from 0.01 V/nm to 1 V/nm, total amount of emission (area under the curve) will increase due to the reduction of the potential barrier, but the location of the peak remains unchanged [see Fig. 3(a)]. By increasing $T$ from 5 K to 300 K, more electrons with higher energy will emit due to the broadening in the Fermi-Dirac distribution, and thus, the peak of the distribution will shift to the left [see Fig. 3(b)]. Lastly, Fig. 3(c) shows that the range of the distribution becomes wider with higher values of $E_f$, as we have more electrons emitted over a wider energy range. These calculated results could be tested against experiment to confirm Klein tunneling as compared to the standard distributions based on the FN law.

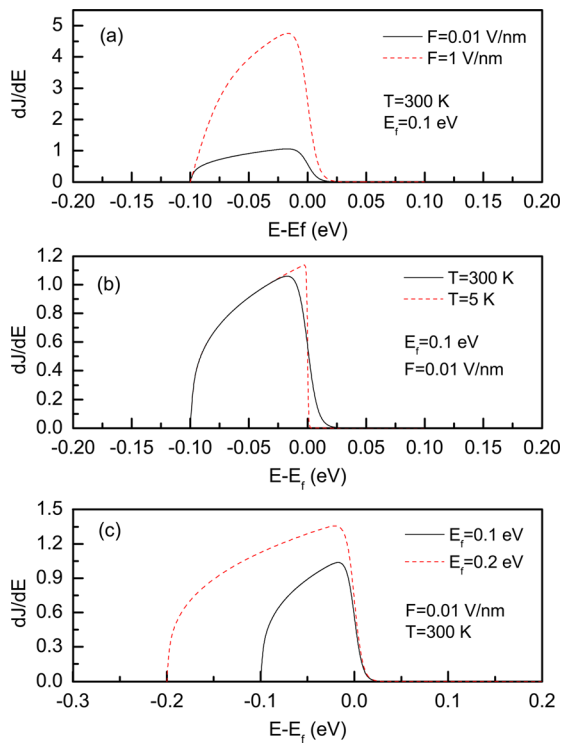


FIG. 3. (Color online) The normalized energy distribution of the emitted electrons for different (a) local field $F = 0.01$ and 1 V/nm; (b) temperature $T = 5$ and 300 K; and (c) Fermi energy $E_f = 0.1$ and 0.2 eV. The normalized constant is at $T = 300$ K, $F = 0.01$ V/nm, and $E_f = 0.1$ eV (see solid lines).

Due to the capability of high current emission at low turn-on voltage from the Klein tunneling model studied here, the space charge effects may become important. However, a model to show the transition from the Klein tunneling field emission model (proposed here) to the space charge limited (SCL) current will require a multi-dimensional quantum relativistic treatment, to include the effects of extremely small emission area, quantum, and relativistic, which had been studied before but in separate independent models.[19–22] We also speculate that if multiple-layers of graphene sheet is considered in the model, the emission characteristic will recover to FN law as expected for a bulk material. Lastly, the assumption of using the same classical image charge potential (of the FN law) for graphite field emission will require further investigation, but we believe that the new scaling reported here is due to Klein tunneling rather than the profile of the potential barrier. Note the above three issues will require follow-on works and are beyond the scope of this paper.

This work was supported by a Singapore MOE grant (2008-T2-01-033), USA AOARD grant (10-4110).

[1]K. S. Novoselov, A. K. Geim, S. V. Morozov, D. Jiang, Y. Zhang, S. V. Dubonos, I. V. Gregorieva, and A. A. Firsov, Science **306**, 666 (2004).
[2]A. H. C. Neto, F. Guinea, N. M. R. Peres, K. S. Novoselov, and A. K. Geim, Rev. Mod. Phys. **81**, 109 (2009).
[3]U. A. Palnitkar, R. V. Kashid, M. A. More, D. S. Joag, L. S. Panchakalar, and C. N. R. Rao, Appl. Phys. Lett. **97**, 063102 (2010).
[4]A. Malesevic, R. Kemps, A. Vanhulsel, M. P. Chowdhury, A. Volodin, and C. V. Haesendonck, J. Appl. Phys. **104**, 084301 (2008).
[5]S. Wang, J. Wang, P. Miraldo, M. Zqhu, R. Outlaw, K. Hou, X. Zhou, B. C. Holloway, D. Manos, T. Tyler, et al., Appl. Phys. Lett. **97**, 183103 (2006).
[6]Z. S. Wu, S. F. Pei, W. C. Ren, D. M. Tang, L. B. Gao, B. L. Liu, F. Li, C. Liu, and H. M. Cheng, Adv. Mater. **21**, 1756 (2009).
[7]K. Uppireddi, C. V. Rao, Y. Ishikawa, B. R. Weiner, and G. Morell, Appl. Phys. Lett. **97**, 062106 (2010).
[8]G. Eda, H. E. Unalan, N. Rupesinghe, G. A. J. Amaratunga, and M. Chhowalla, Appl. Phys. Lett. **93**, 233502 (2008).
[9]H. M. Wang, Z. Zheng, Y. Y. Wang, J. J. Qiu, Z. B. Guo, Z. X. Shen, and T. Yu, Appl. Phys. Lett. **96**, 023106 (2010).
[10]R. H. Fowler and L. Nordheim, Proc. R. Soc. London, Ser. A **119**, 683 (1928).
[11]O. Klein, Z. Phys. **53**, 157 (1929).
[12]M. I. Katsnelson, K. S. Novoselov, and A. K. Geim, Nat. Phys. **2**, 620 (2006).
[13]R. Miller, Y. Y. Lau, and J. H. Booske, Appl. Phys. Lett. **91**, 074105 (2007).
[14]F. Guo, A. Mukhopadhyay, B. W. Sheldon, and R. H. Hurt, Adv. Mater. **23**, 508 (2011).
[15]K. L. Jensen, J. Vac. Sci. Technol. B **13**(2), 516 (1995).
[16]O. K. Reity, V. Y. Lazur, and S. I. Myhalyna, Proc. Inst. Math. NAS Ukraine **50**, 1429 (2004).
[17]V. Y. Lazur, O. K. Reity, and V. V. Rubish, Theor. Math. Phys. **143**, 559 (2005).
[18]L. Wu and L. K. Ang, Appl. Phys. Lett. **89**, 133503 (2006).
[19]Y. Y. Lau, Phys. Rev. Lett. **87**, 278301 (2001).
[20]R. J. Umstattd and J. W. Luginsland, Phys. Rev. Lett. **87**, 145002 (2001).
[21]L. K. Ang, T. J. T. Kwan, and Y. Y. Lau, Phys. Rev. Lett. **91**, 208303 (2003).
[22]L. K. Ang and P. Zhang, Phys. Rev. Lett. **98**, 164802 (2007).